Dalton Transactions

PAPER

View Article Online
View Journal | View Issue

CrossMark click for updates

Cite this: *Dalton Trans.*, 2016, **45**, 15500

A ligand substituted tungsten iodide cluster: luminescence *vs.* singlet oxygen production†

Lara Riehl,[a] Alexander Seyboldt,[a] Markus Ströbele,[a] David Enseling,[b] Thomas Jüstel,[b] Michael Westberg,[c] Peter R. Ogilby[c] and H.-Jürgen Meyer*[a]

Received 20th June 2016,
Accepted 4th September 2016

DOI: 10.1039/c6dt02471h

www.rsc.org/dalton

Octahedral tungsten iodide clusters equipped with apical ligands (L) are synthesized to implement substantial photophysical properties. The $[W_6I_8(CF_3COO)_6]^{2-}$ cluster reported herein is the first example of a family of ligand substituted $[W_6I_8L_6]^{2-}$ clusters. Such compounds are expected to exhibit a rich photochemistry in which the apical ligands play a crucial role. The versatile solid state and solution phase photophysical properties of $(TBA)_2[W_6I_8(CF_3COO)_6]$ described herein parallel characteristics obtained in some photophysically active organic compounds, including a broad absorption in the UV/VIS region. Upon irradiation of this compound, a broad red emission is observed in the VIS/NIR region resulting from excited triplet states, and singlet oxygen ($a^1\Delta_g$) is generated in the presence of O_2.

Introduction

Optical materials are an essential part of our daily life; they offer attractive and energy-efficient applications in photocatalysis,[1] sensing,[2] lighting,[3] and solar energy harvesting,[4] for example. Thus, photoactive materials and studies of the properties of such materials with an eye to new developments are important.

For the past decades, the electronic structure and photophysical properties of Mo_6Cl_{12} based compounds have been studied.[5] The structure of the $[Mo_6Cl_{14}]^{2-}$ ion is based on an octahedral molybdenum cluster core carrying eight inner (i = innen) face-capping and six outer (a = außen) apical chloride ligands making up a $[Mo_6Cl_8^iCl_6^a]^{2-}$ ion which resembles the prototypical structure for many cluster compounds. Cluster compounds of this type are remarkably stable in solution and in the solid state. However, their apical ligands are always more weakly bound, allowing a broad substitutional chemistry for terminal ligands (L).

Considerable attention has focused on the structures and photophysical properties of octahedral metal cluster compounds $[M_6X_8L_6]^{n-}$ with M = Mo, X = halide, and M = Re, X = S, Se or Te, containing inorganic or organic ligands (L).[6]

Octahedral rhenium chalcogenide clusters, developed almost simultaneously in 1999 by the groups of Kitamura,[7] Batail[8] and Nocera[9] are showing versatile potential in optical applications.[10] Likewise, a number of ligand substituted octahedral molybdenum clusters, such as $(TBA)_2[Mo_6I_8(C_3F_7COO)_6]$[11] and $(TBA)_2[Mo_6I_8(CF_3COO)_6]$[12] (TBA = tetrabutyl ammonium), exhibit remarkable photophysical properties.[13]

The aforementioned metal chalcogenide and metal halide compounds have broad absorption bands in the UV-VIS region and emit in the red VIS/NIR region of the electromagnetic spectrum. It is clear that the photoexcitation involves an S_0 to S_m transition, followed by intersystem crossing (ISC) into triplet states.[14] Phosphorescence quenching obtained in the presence of molecular oxygen is, at least partially, explained by energy transfer with the formation of singlet oxygen, $O_2(a^1\Delta_g)$,[15] as shown in Fig. 1.

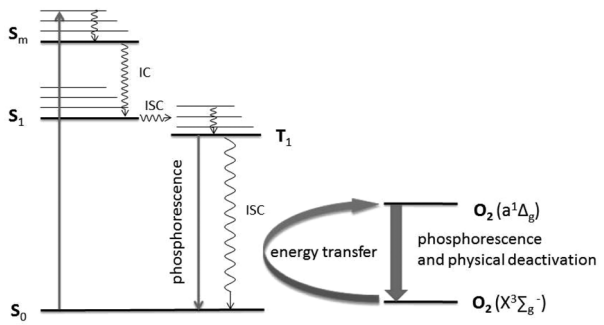

Fig. 1 Electronic transitions and singlet oxygen generation ($a^1\Delta_g$) in $[M_6X_8L_6]^{2-}$ type clusters following a modified Jablonski-Diagram.[16]

[a]*Abteilung für Festkörperchemie und Theoretische Anorganische Chemie, Institut für Anorganische Chemie, Universität Tübingen, Auf der Morgenstelle 18, 72076 Tübingen, Germany. E-mail: juergen.meyer@uni-tuebingen.de*
[b]*Labor für Angewandte Materialwissenschaften, Fachhochschule Münster, Stegerwaldstrasse 39, 48565 Steinfurt, Germany. E-mail: tj@fh-muenster.de*
[c]*Department of Chemistry, Aarhus University, Langelandsgade 140, 8000 Aarhus, Denmark. E-mail: progilby@chem.au.dk*

†Electronic supplementary information (ESI) available. CCDC 1063061 and 1479582. For ESI and crystallographic data in CIF or other electronic format see DOI: 10.1039/c6dt02471h

The photophysical and electrochemical properties of $[M_6X_8L_6]^{2-}$ cluster compounds can be tuned by substitutions of inner ligands (X) as well as outer organic or inorganic ligands (L).[12,14c,17] The perspectives of ligand exchange reactions in $[M_6X_8L_6]$ clusters and the influence of apical ligands with respect to the $S_0 \rightarrow S_1$ excitation, described as ligand → metal charge transfer (LMCT)[6b,18] and consequent photophysical effects are not fully explored. However, there is high potential and interest in $[M_6X_8L_6]$ cluster compounds regarding applications in the fields of oxygen sensing,[5c] catalysis,[19] photocatalysis,[20] photoreduction of CO_2,[21] luminescent nanoparticles,[22] organic synthesis,[23] and photodynamic therapy,[24] for example.

Molybdenum clusters with the general formula $[Mo_6X_8L_6]^{2-}$ have shown excellent luminescence properties. For the compound $(TBA)_2[Mo_6I_8(CF_3COO)_6]$, a luminescence quantum yield (Φ_L) near 1 was reported in (oxygen-free) acetonitrile solution, and a quantum yield of 0.84 was reported for the sensitized production of singlet oxygen (Φ_Δ) in the presence of oxygen.[12,25]

Corresponding tungsten iodide compounds $[W_6I_8L_6]^{2-}$ remained absent until now. One reason is that there has been no appropriate synthesis available for the preparation of a binary tungsten iodide which could serve as a starting material (*e.g.* W_6I_{12}), although particularly strong luminescence properties of tungsten iodides, among $[W_6X_6X'_6]^{2-}$ clusters with X, X′ = Cl, Br, I, have been observed.[26] We here report the synthesis and photophysical characterization of a ligand substituted $[W_6I_8L_6]^{2-}$ cluster compound.

Results and discussion

The development of a new synthetic route for tungsten iodides based on a halide exchange reaction of WCl_6 with SiI_4 enable us to generate tungsten iodide in large scale, based on $W_3I_8{\cdot}nI_2$ with n = 0, $\frac{1}{2}$, 2.[27] The octahedral cluster compound $Cs_2[W_6I_{14}]$ is prepared by thermal conversion of appropriate amounts of W_3I_{12} and CsI in a sealed silica container near 550 °C.[28]

An improved solubility in organic solvents is obtained by cation substitution reaction with (TBA)I, performed in a two phase solvent mixture (DCM : water).[29] $(TBA)_2[W_6I_{14}]$ is obtained as a bright yellow crystalline powder after phase separation and filtration from the organic phase. The crystal structure of $(TBA)_2[W_6I_{14}]$ was refined with the monoclinic space group $P2_1/n$ from X-ray diffraction data with the FullProf program package.[30] Average W–W distances of the octahedral cluster are 266.1 pm, W–I distances with inner iodide ligands average at 278.3 pm, and corresponding distances with apical iodide ligands are 285.5 pm.

$(TBA)_2[W_6I_{14}]$ as well as the starting material $A_2[W_6I_{14}]$ are key compounds for the development of ligand substituted $[W_6I_8L_6]^{2-}$ cluster compounds with organic or inorganic ligands (L). Because it is unknown which ligand will give rise to the most promising photophysical properties with tungsten iodide clusters, we first attempted the preparation of a trifluoroacetate compound, as has been reported for the parent molybdenum compound.[12] The exchange reaction of six outer iodide ligands in $[W_6I_8{}^iI_6{}^a]^{2-}$ is performed with excess silver trifluoroacetate (1 : 7 molar ratio) in dichloromethane under stirring at room temperature for three days in the dark, following the scheme given in Fig. 2.

$(TBA)_2[W_6I_8(CF_3COO)_6]$ is obtained as an orange colored crystalline solid with 79% yield. Good quality single crystals for X-ray structure analysis are grown from a saturated solution in ethanol by overlaying with pentane.

The identity of the cluster was confirmed from a (ESI) mass spectrum in methanol solution (Bruker Esquire 3000 plus), yielding mass peaks which are assigned to m/z = 3037.6 $\{(TBA)[W_6I_8(CF_3COO)_6]\}^-$, and m/z = 2682.5 $\{[W_6I_8(CF_3COO)_5]\}^-$ fragments.

$(TBA)_2[W_6I_8(CF_3COO)_6]$ crystallizes with the triclinic space group $P\bar{1}$. $[W_6I_8(CF_3COO)_6]^{2-}$ ions are arranged in the *bc*-plane of the crystal, following the motive of a hexagonal closed packed layer, with a primitive stacking sequence along the *b*-axis direction. TBA ions can be approximated to occupy trigonal prismatic voids made up by the arrangement of clusters (Fig. 3).

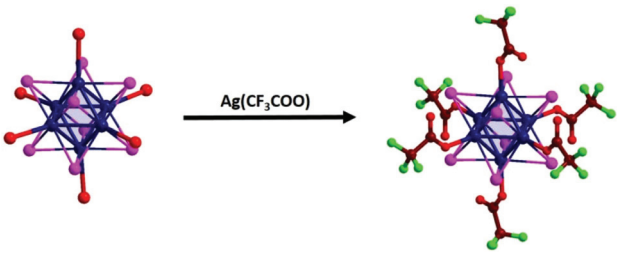

Fig. 2 Exchange reaction of outer (a) iodide ligands in $[W_6I_8{}^iI_6{}^a]^{2-}$ by trifluoroacetate with the formation of $[W_6I_8(CF_3COO)_6]^{2-}$.

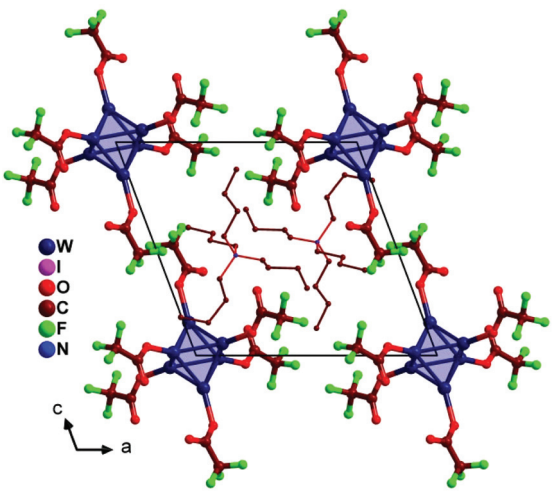

Fig. 3 Crystal structure of $(TBA)_2[W_6I_8(CF_3COO)_6]$ projected on the *ac*-plane (iodide ligands are omitted).

Tungsten atoms in the centrosymmetric $[W_6I_8(CF_3COO)_6]^{2-}$ cluster are arranged to form an octahedral arrangement with W–W distances ranging between 264.67(4) and 265.80(5) pm. Triangular cluster faces are capped by inner iodide ligands with W–I distances ranging from 278.48(6) to 282.24(6) pm. Three crystallographically distinct trifluoroacetate ligands appear in $(TBA)_2[W_6I_8(CF_3COO)_6]$ forming W–O–C angles of 135.1(6)°, 136.8(6)° and 134.8(6)° with tungsten atoms of the cluster. C–C distances within trifluoroacetate ligands range from 149(1) to 152(1) pm, consistent with a C–C single bond (148 pm), and C–C–F angles vary from 110.7(9)° to 115.2(12)°.

Crystalline powders of $(TBA)_2[W_6I_8(CF_3COO)_6]$ appear orange and show red-orange phosphorescence when exposed to UV radiation (Fig. 4). The phosphorescence can be considered an intrinsic property of the $[W_6I_8(CF_3COO)_6]^{2-}$ cluster anion, and the relative emission intensities of the crystalline powder continuously increases after milling with a highly reflective (inert) solid such as $BaSO_4$. The quantum yield (Φ_P) of $(TBA)_2[W_6I_8(CF_3COO)_6]$ is 4% as a pure microcrystalline powder, and 23% after milling with $BaSO_4$, as determined in an integrating sphere in air.[31] The increase of the luminescence intensity may be understood as a result of increased separation of clusters, which are considered as phosphorescence centers. This is in line with the observation of a considerably higher phosphorescence intensity once $[W_6I_8(CF_3COO)_6]^{2-}$ cluster anions are transferred into solution under inert atmosphere, as will be shown later.

The emission spectrum of microcrystalline $(TBA)_2[W_6I_8(CF_3COO)_6$ shows a broad emission band at 660 nm (1.88 eV) with a full width at half maximum (FWHM) of 0.43 eV (~3500 cm^{-1}) when excited with 400 nm (Fig. 5). The excitation spectrum of this emission band shows a maximum at 400 nm with full width at half maximum (FWHM) of 2.48 eV (~20 000 cm^{-1}). A similar behavior is reported for $(TBA)_2[Mo_6I_8(CF_3COO)_6]$, which was prepared as a reference material.[12]

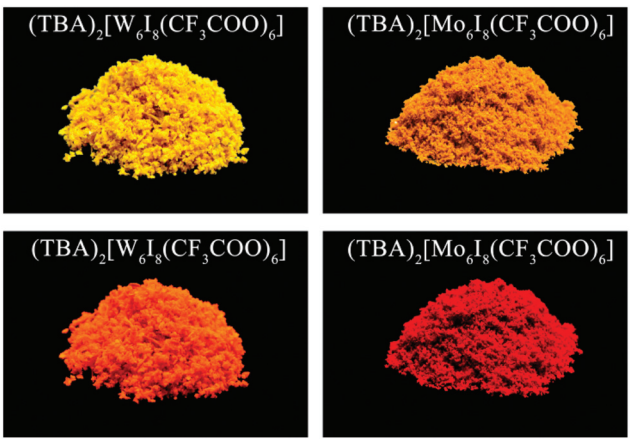

Fig. 4 Crystalline powders of $(TBA)_2[W_6I_8(CF_3COO)_6]$ (left) and $(TBA)_2[Mo_6I_8(CF_3COO)_6]$ (right) under ambient light (top) and under UV radiation (366 nm, bottom).

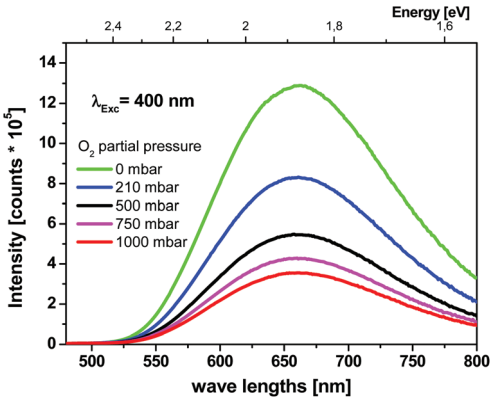

Fig. 5 Emission spectra of microcrystalline $(TBA)_2[W_6I_8(CF_3COO)_6]$ powder under several oxygen partial pressures ($\lambda_{em,max}$ = 660 nm).

The large FWHM combined with a large Stokes shift of 1.12 eV (~9000 cm^{-1}) of $(TBA)_2[W_6I_8(CF_3COO)_6]$ can be related to a charge transfer transition.[32] The phosphorescence of both compounds is quenched in the presence of oxygen. Emission spectra of $(TBA)_2[W_6I_8(CF_3COO)_6]$ recorded as a function of the oxygen partial pressure are shown in Fig. 5. The phosphorescence intensity as well as the decay time decrease with increasing oxygen partial pressure. The decay time of $(TBA)_2[W_6I_8(CF_3COO)_6]$ in pure nitrogen is 29.2 μs and in pure oxygen 9.9 μs (see ESI†). As the oxygen partial pressure is changed, the photoluminescence intensity as well as the decay time show reversibility within the limit of error of our measurements.

Because the quantum yield of emission is correlated with the decay time ($\Phi = \tau/\tau_r$, where τ is the measured decay time and τ_r the decay time for the radiative transition),[33] the relative decay time, τ, can be used to predict the relative change of the quantum yield.

Accordingly, the relative quantum yield of $(TBA)_2[W_6I_8(CF_3COO)_6]$ emission in pure oxygen atmosphere drops to 34% of the value obtained in pure nitrogen. A similar behavior is observed for $(TBA)_2[Mo_6I_8(CF_3COO)_6]$, where the relative quantum yield drops to 5%. The bimolecular oxygen-mediated quenching processes have been quantified *via* Stern–Volmer analysis (see Fig. 6). These results imply that this type of cluster compound could be considered as an oxygen sensor. Moreover, the oxygen mediated quenching of the phosphorescent triplet state could potentially lead to the formation of singlet oxygen, $O_2(a^1\Delta_g)$ (Fig. 1).

The photophysics of the compounds dissolved in acetonitrile was investigated (Table 2). Both clusters show a red-shifted emission spectrum, and the emission spectrum of $(TBA)_2[W_6I_8(CF_3COO)_6]$ is particularly broad and extends into the NIR (see ESI†). Phosphorescence lifetimes were determined at three different oxygen concentrations. From these lifetimes, it is possible to calculate the bimolecular rate constant for quenching of the triplet state by oxygen, k_q. Even though the quenching process is not diffusion-limited, it can be calculated that more than 98% of the triplet states are

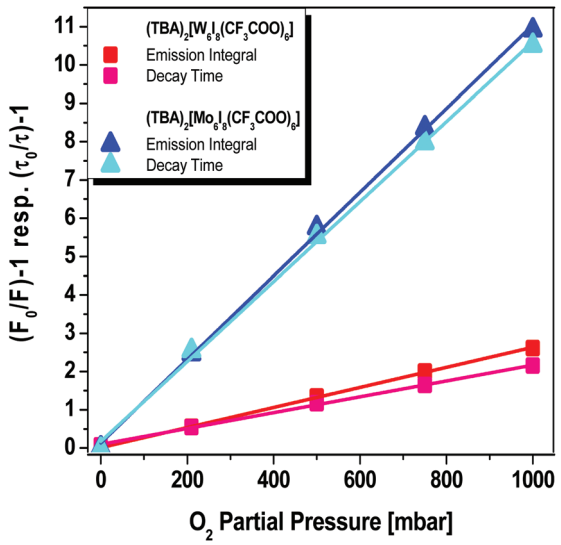

Fig. 6 Stern–Volmer plots of the emission integrals as well as the decay times of microcrystalline $(TBA)_2[W_6I_8(CF_3COO)_6]$ and $(TBA)_2[Mo_6I_8(CF_3COO)_6]$ powder as a function of oxygen partial pressures.

quenched by oxygen under aerated conditions (f_T, Table 2). This is clearly reflected in the very small phosphorescence quantum yields under these conditions.

In order to check if this quenching process involves energy transfer to ground-state oxygen ($X^3\Sigma_g^-$), the quantum yields of $O_2(a^1\Delta_g)$ formation were determined *via* the characteristic 1275 nm phosphorescence signal from $O_2(a^1\Delta_g)$.[16] Indeed, both clusters ($[W_6I_8(CF_3COO)_6]^{2-}$ and $[Mo_6I_8(CF_3COO)_6]^{2-}$) are efficient $O_2(a^1\Delta_g)$ photosensitizers under aerated and oxygenated conditions (Table 2). However, for both clusters the observation that the singlet oxygen quantum yield is lower than the fraction of triplet states quenched by oxygen ($\Phi_\Delta < f_T$) implies that (1) the triplet quantum yield may be below unity and/or (2) some of the encounter complexes between oxygen and the hexanuclear clusters decay *via* a non-radiative mechanism instead of energy transfer to make singlet oxygen. Such mechanisms often dominate for photosensitizers with appreciable charge-transfer character.[34] An interesting direction for future studies could therefore be to systematically develop $[W_6I_8L_6]^{2-}$ cluster compounds and to investigate the effect of ligand-exchange on the singlet oxygen yields and charge-transfer character in the complexes.[34c,d] Furthermore, solvent-effects could potentially also tune the excited state properties of the clusters.[34a,35]

The functionalization of photophysically active clusters by means of deposition, incorporation, and encapsulation is a logical need for further applications.[10]

Experimental section

Materials and methods

Unless otherwise noted, all reactions were carried out in an argon atmosphere in dried and degassed solvents using Schlenk techniques. All solvents were purchased from Sigma-Aldrich, dried and degassed with an MBraun SPS-800 solvent purification system. Chemicals used were obtained from commercial suppliers and were used without further purification.

X-ray crystallographic studies

$Cs_2[W_6I_{14}]$. An orange single-crystal of $Cs_2[W_6I_{14}]$ was measured with a single-crystal X-ray diffractometer (STOE-IPDS II) at 25 °C using Mo-K_α (λ = 0.71073 Å) radiation. Raw data intensities were corrected for Lorentz factors and polarization by the IPDS software. Absorption effects were corrected by the X-Red/X-Shape program of the STOE software. Crystal structure solutions were performed with direct methods (SHELXS), followed by full-matrix least square structure refinements with SHELXL-2014.[36] Results are shown in the ESI.†

Further details of the crystal structure investigations may be obtained from the Fachinformationszentrum Karlsruhe, 76344 Eggenstein-Leopoldshafen, Germany (Fax: +49 7247-808-666; E-mail: crysdata@fiz-karlsruhe.de, http://www.fiz-karlsruhe.de/request for deposited data.html) on quoting the depository number CSD 429577 for $Cs_2[W_6I_{14}]$.

$(TBA)_2[W_6I_{14}]$. Orange crystalline powders were measured and characterized by X-ray powder diffraction (StadiP, Stoe, Darmstadt, Ge-monochromatic Cu-$K\alpha_1$ radiation). The crystal structures were indexed isotypically to $(TBA)_2[Mo_6I_{14}]$,[37] and refined by global refinement using the WinPlotr (FullProf Suite[38]). Final R indices and general parameters are given in the ESI.†

$(TBA)_2[W_6I_8(CF_3COO)_6]$. An orange single-crystal of $(TBA)_2[W_6I_8(CF_3COO)_6]$ was measured with a single-crystal X-ray diffractometer (STOE-IPDS II) at −40 °C using Mo-K_α (λ = 0.71073 Å) radiation. Absorption effects were corrected by the X-Red/X-Shape program of the STOE software. The crystal structure solution and refinement was performed with direct methods (SHELXS) and least square refinements on F^2 (SHELXL). Some results are shown in Table 1.

Table 1 Selected crystallographic data for $(TBA)_2[W_6I_8(CF_3COO)_6]$

	$(TBA)_2[W_6I_8(CF_3COO)_6]$
Empirical formula	$C_{44}H_{72}F_{18}I_8N_2O_{12}W_6$
Formula weight	3281.33
Crystal system	$P\bar{1}$
a, b, c (pm)	1308.62(4), 1321.46(4), 1335.44(4)
α, β, γ	114.963(2)°, 102.910(3)°, 102.138(3)°
V (nm^3)	1.9157(1)
Z, D_x (g cm^{-3})	1, 2.844
μ (mm^{-1})	12.285
F(000)	1476
Crystal size (mm)	0.2 × 0.1 × 0.1
T_{max}, T_{min}	0.4031, 0.1180
Number of measured and independent reflections	17 913, 6690
R_{int}	0.0188
Θ_{max}	25.026°
Final R indices [$I > 2\sigma(I)$]	R_1 = 0.0348, wR_2 = 0.0763
Largest diff. peak and hole	0.667 and −0.592 e Å^{-3}

Table 2 Photophysical data recorded in acetonitrile under varying oxygen concentrations (τ_T = triplet lifetime; k_q = bimolecular quenching constant; f_T = fraction of triplet state quenched by oxygen; Φ_P = quantum yield of phosphorescence; Φ_Δ = quantum yield of singlet oxygen formation)

		$(TBA)_2[W_6I_8(CF_3COO)_6]$	$(TBA)_2[Mo_6I_8(CF_3COO)_6]$
$\lambda_{em,max}$ [nm]		677 ± 2	675 ± 2
τ_T [μs]	N_2	36 ± 1	300 ± 10
	Air	1.08 ± 0.02	1.84 ± 0.03
	O_2	0.23 ± 0.01	0.38 ± 0.01
k_q [10^8 $M^{-1}s^{-1}$]		3.7 ± 0.1	2.3 ± 0.1
f_T	Air	0.98 ± 0.01	0.99 ± 0.01
Φ_P	Air	0.015 ± 0.003	0.004 ± 0.001
Φ_Δ	Air	0.81 ± 0.06	0.84 ± 0.07
	O_2	0.81 ± 0.06	0.85 ± 0.07

Crystallographic data (including structure factors) for $(TBA)_2[W_6I_{14}]$ and $(TBA)_2[W_6I_8(CF_3COO)_6]$ has been deposited with the Cambridge Crystallographic Data Centre, CCDC, 12 Union Road, Cambridge CB12EZ, UK. Copies of the data can be obtained free of charge on quoting the depository number CCDC 1063061 for $(TBA)_2[W_6I_{14}]$ and CCDC 1479582 for $(TBA)_2[W_6I_8(CF_3COO)_6]$.

Solid state photoluminescence measurements

Emission spectra and decay curves were collected with a fluorescence spectrometer FLS920 (Edinburgh Instruments) equipped with a 450 W ozone-free xenon arc lamp (OSRAM) for the emission scan and a μF920H flash lamp for the decay curve. The sample chamber was installed with a mirror optic for powder samples. For detection, a R2658P single-photon counting photomultiplier tube (Hamamatsu) was used. All luminescence spectra were recorded with a spectral resolution of 1 nm, a dwell time of 0.4 s in 1 nm steps, and three repeats. The sample was in a gas flow sample holder under ambient pressure (about 1 bar) and was perfused with nitrogen, air, oxygen and oxygen–nitrogen mixtures 50/50 and 75/25.

Solution phase spectroscopy

The compounds were dissolved in HPLC-grade acetonitrile (Sigma-Aldrich). Solutions were saturated with N_2 or O_2 by bubbling with the respective gas for at least 30 min. Phenalenone and 4-(dicyanomethylene)-2-methyl-6-(4-dimethylaminostyryl)-4*H*-pyran (Sigma-Aldrich) was used as received. All experiments were performed in 1 cm quartz cuvettes.

Equipment and methods used to determine singlet oxygen quantum yields, Φ_Δ, have been described in detail elsewhere.[39] In short, the chromophores were excited using fs-laser pulses centered at 383 nm, and photosensitization of $O_2(a^1\Delta_g)$ was follow *via* the characteristic phosphorescence signal at ~1275 nm. This signal was isolated using a 1064 nm long-pass filter combined with a 1290/80 nm band-pass filter in front of a VIS/NIR-sensitive PMT. Phenalenone dissolved in acetonitrile was used as the reference sensitizer (Φ_Δ = 0.99 ± 0.03).[40]

Phosphorescence lifetimes of the tungsten cluster were measured using the same instruments as described above. Excitation was done at either 383 or 419 nm, and the phosphorescence signals were isolated using a 650/40 nm band-pass filter. The bimolecular rate constant for quenching of the cluster triplet state by oxygen, k_q, was calculated using a concentration of oxygen in air-saturated acetonitrile of 2.42 mM.[41]

Phosphorescence quantum yields of the cluster were measured using a home-built setup that allows for acquisition of emission spectra extending to 880 nm. This setup uses the same fs-laser as described above, but for these measurements the detection unit is an Andor Technology, iStar 320 T, ICCD camera connected to an Andor Technology, Shamrock 303i, spectrograph. The detection path is positioned at a 90 degrees angle relative to the excitation path. The detection unit has been intensity calibrated. 4-(Dicyanomethylene)-2-methyl-6-(4-dimethylaminostyryl)-4*H*-pyran in acetonitrile (Φ_P = 0.44 ± 0.05)[42] and absolute ethanol (Φ_P = 0.435 ± 0.022)[43] was used as reference standard.

Synthesis of $Cs_2[W_6I_{14}]$ and $(TBA)_2[W_6I_{14}]$

$$2W_3I_{12} + 2CsI \rightarrow Cs_2[W_6I_{14}] + 6I_2$$

W_3I_{12} (1.2 g, 0.58 mmol) was grounded with CsI (150.3 mg, 0.58 mmol) and filled into a silica ampule. This ampule was flame sealed under vacuum and placed in a tube furnace at 550 °C for 24 h. The product was obtained as a brown powder in quantitative yield.

$$Cs_2[W_6I_{14}] + 2(TBA)I \rightarrow (TBA)_2[W_6I_{14}] + 2CsI$$

769 mg (0.24 mmol) $Cs_2[W_6I_{14}]$ were added to a solution of 270 mg (0.73 mmol) (TBA)I in 100 mL CH_2Cl_2/H_2O (1 : 1). After stirring the mixture for 48 h the organic phase was separated and filtered. The solvent was removed and the precipitate was washed three times with distilled water. The orange solid was then again dissolved in DCM and again filtered. After removing the solvent $(TBA)_2[W_6I_{14}]$ was obtained as an orange solid in 79% yield.

Synthesis of $(TBA)_2[W_6I_8(CF_3COO)_6]$

$$(TBA)_2[W_6I_{14}] + 6Ag(CF_3COO) \rightarrow (TBA)_2[W_6I_8(CF_3COO)_6] + 6AgI$$

$(TBA)_2[W_6I_{14}]$ (150 mg, 0.044 mmol) was diluted in 35 mL dried DCM and $Ag(CF_3COO)$ (68.9 mg, 0.312 mmol) was added. The reaction was stirred for 72 h in the dark. After filtration the solvent was removed and the brown solid was dissolved in 10 mL of cold ethanol and filtered again. Afterwards the solution was refluxed for 2 h to agglomerate the silver nanoparticles and again filtered. The solvent was then removed *in vacuo* and the product $(TBA)_2[W_6I_8(CF_3COO)_6]$ was obtained as a yellow powder in 69% yield. To obtain single crystals suitable for X-ray diffraction a saturated solution of the compound in ethanol was over layered with *n*-pentane and

stored at 3.5 °C. The compound remains stable in moist air, as could be shown by unchanged XRD patterns and unchanged luminescence properties after being exposed to air for several months.

ESI-MS: m/z = 3037.6 $\{(TBA)[W_6I_8(CF_3COO)_6]\}^-$; m/z = 2682.5 $\{[W_6I_8(CF_3COO)_5]\}^-$

Conclusions

$(TBA)_2[W_6I_8(CF_3COO)_6]$ represents the first tungsten iodide cluster compound of a growing family of ligand substituted tungsten iodide clusters containing $[W_6I_8L_6]^{2-}$ ions that are currently developed in Tübingen. The present compound exhibits remarkable stability in moist air. Recorded photophysical properties parallel those obtained for parent molybdenum clusters, represented by a red phosphorescence in solid state and in solution. The phosphorescence emission intensity is quenched with increasing concentration of molecular oxygen, with the formation of singlet oxygen in high yield.

Acknowledgements

We are indebted to Mr Thorsten Hummel for the preparation of $Cs_2[W_6I_{14}]$ and to Dr Danuta Dutczak for the photographic art work.

Notes and references

1 J. Liqiang, Q. Yichun, W. Baiqi, L. Shudan, J. Baojiang, Y. Libin, F. Wei, F. Honggang and S. Jiazhong, *Sol. Energy Mater. Sol. Cells*, 2006, **90**, 1773–1787.
2 Y. Feng, J. Cheng, L. Zhou, X. Zhou and H. Xiang, *Analyst*, 2012, **137**, 4885–4901.
3 T. Jüstel, H. Nikol and C. Ronda, *Angew. Chem., Int. Ed.*, 1998, **37**, 3084–3103.
4 M. Grätzel, *Inorg. Chem.*, 2005, **44**, 6841–6851.
5 (*a*) J. C. Sheldon, *J. Chem. Soc.*, 1960, 3106; (*b*) J. E. Fergusson, B. H. Robinson and C. J. Wilkins, *J. Chem. Soc. A*, 1967, 486–490; (*c*) D. J. Osborn and G. L. Baker, *J. Sol–Gel Sci. Technol.*, 2005, **36**, 5–10.
6 (*a*) W. A. Rabanal-León, J. A. Murillo-López, D. Páez-Hernández and R. Arratia-Pérez, *J. Phys. Chem. A*, 2014, **118**, 11083–11089; (*b*) R. Ramirez-Tagle and R. Arratia-Pérez, *Chem. Phys. Lett.*, 2008, **460**, 438–441.
7 T. Yoshimura, S. Ishizaka, K. Umakoshi, Y. Sasaki, H.-B. Kim and N. Kitamura, *Chem. Lett.*, 1999, **28**, 697–698.
8 C. Guilbaud, A. Deluzet, B. Domercq, P. Molinie, K. Boubekeur, P. Batail and C. Coulon, *Chem. Commun.*, 1999, 1867–1868.
9 T. G. Gray, C. M. Rudzinski, D. G. Nocera and R. H. Holm, *Inorg. Chem.*, 1999, **38**, 5932–5933.
10 S. Cordier, Y. Molard, K. A. Brylev, Y. Mironov, F. Grasset, B. Fabre and N. G. Naumov, *J. Cluster Sci.*, 2015, **26**, 53–81.
11 M. N. Sokolov, M. A. Mihailov, E. V. Peresypkina, K. A. Brylev, N. Kitamura and V. P. Fedin, *Dalton Trans.*, 2011, **40**, 6375–6377.
12 K. Kaplan, P. Kubát, M. Dusek, K. Fejfarvová, V. Sícha, J. Mosinger and K. Lang, *Eur. J. Inorg. Chem.*, 2012, 3107–3111.
13 (*a*) K. Harder and W. Preetz, *Z. Anorg. Allg. Chem.*, 1992, **612**, 97–100; (*b*) W. Preetz, G. Peters and D. Bublitz, *Chem. Rev.*, 1996, **96**, 977–1026.
14 (*a*) T. Azumi and Y. Saito, *J. Phys. Chem.*, 1988, **92**, 1715–1721; (*b*) A. Guirauden, I. Johannsen, P. Batail and C. Coulon, *Inorg. Chem.*, 1993, **32**, 2446–2452; (*c*) A. W. Maverick, J. S. Najdzionek, D. MacKenzie, D. G. Nocera and H. B. Gray, *J. Am. Chem. Soc.*, 1983, **105**, 1878–1882; (*d*) A. W. Maverick and H. B. Gray, *J. Am. Chem. Soc.*, 1981, **103**, 1298–1300; (*e*) T. C. Zietlow, M. D. Hopkins and H. B. Gray, *J. Solid State Chem.*, 1985, **57**, 112–119.
15 J. A. Jackson, C. Turro, M. D. Newsham and D. G. Nocera, *J. Phys. Chem.*, 1990, **94**, 4500.
16 P. R. Ogilby, *Chem. Soc. Rev.*, 2010, **39**, 3181–3209.
17 T. C. Zietlow, M. D. Hopkins and H. B. Gray, *J. Solid State Chem.*, 1985, **57**, 112–119.
18 (*a*) L. M. Robinson, R. L. Bain, D. F. Shriver and D. E. Ellis, *Inorg. Chem.*, 1995, **34**, 5588–5596; (*b*) L. F. Szczepura, J. A. Edwards and D. L. Cedeño, *J. Cluster Sci.*, 2009, **20**, 105–112.
19 S. Kamiguchi, S. Nagashima and T. Chihara, *Metals*, 2014, **4**, 84.
20 A. Barras, S. Cordier and R. Boukherroub, *Appl. Catal., B*, 2012, **123–124**, 1–8.
21 P. Kumar, S. Kumar, S. Cordier, S. Paofai, R. Boukherroub and S. L. Jain, *RSC Adv.*, 2014, **4**, 10420–10423.
22 T. Aubert, F. Cabello-Hurtado, M.-A. Esnault, C. Neaime, D. Lebret-Chauvel, S. Jeanne, P. Pellen, C. Roiland, L. Le Polles, N. Saito, K. Kimoto, H. Haneda, N. Ohashi, F. Grasset and S. Cordier, *J. Phys. Chem. C*, 2013, **117**, 20154–20163.
23 M. C. DeRosa and R. J. Crutchley, *Coord. Chem. Rev.*, 2002, **233–234**, 351–371.
24 K. Kirakci, P. Kubát, M. Kučeráková, V. Šícha, H. Gbelcová, P. Lovecká, P. Grznárová, T. Ruml and K. Lang, *Inorg. Chim. Acta*, 2016, **441**, 42–49.
25 K. Kirakci, P. Kubát, J. Langmaier, T. Polívka, M. Fuciman, K. Fejfarova and K. Lang, *Dalton Trans.*, 2013, **42**, 7224–7232.
26 T. C. Zietlow, D. G. Nocera and H. B. Gray, *Inorg. Chem.*, 1986, **25**, 1351–1353.
27 M. Ströbele, C. Castro, R. F. Fink and H. J. Meyer, *Angew. Chem., Int. Ed.*, 2016, 4894–4897.
28 (*a*) K. Kirakci, S. Cordier and C. Perrin, *Z. Anorg. Allg. Chem.*, 2005, **631**, 411–416; (*b*) T. Hummel, M. Ströbele, D. Schmid, D. Enseling, T. Jüstel and H.-J. Meyer, *Eur. J. Inorg. Chem.*, 2016, accepted.
29 (*a*) M. K. Simsek, D. Bublitz and W. Preetz, *Z. Anorg. Allg. Chem.*, 1997, **623**, 1885–1891; (*b*) M. K. Simsek and W. Preetz, *Z. Anorg. Allg. Chem.*, 1997, **623**, 515–523.
30 J. Rodríguez-Carvajal, *Phys. B*, 1993, **192**, 55–69.

31 Quantum yields $\bar{1}$ of $(TBA)_2[W_6I_8(CF_3COO)_6]$: ϕ_p = 4% as pure microcrystalline powder; ϕ_p = 23% when dissolved in ethanol grindend with $BaSO_4$.
32 G. Blasse and B. C. Grabmaier, *Luminescent Materials*, Springer-Verlag, Berlin, 1994.
33 G. Gauglitz and T. Vo-Dinh, *Handbook of Spectroscopy*, Wiley-VCH, Weinheim, 2003, vol. 1+2.
34 (*a*) M. Westberg, M. Bregnhøj, A. Blázquez-Castro, T. Breitenbach, M. Etzerodt and P. R. Ogilby, *J. Photochem. Photobiol., A*, 2016, **321**, 297–308; (*b*) C. Schweitzer and R. Schmidt, *Chem. Rev.*, 2003, **103**, 1685–1758; (*c*) A. A. Abdel-Shafi, M. D. Ward and R. Schmidt, *Dalton Trans.*, 2007, 2517–2527; (*d*) P. I. Djurovich, D. Murphy, M. E. Thompson, B. Hernandez, R. Gao, P. L. Hunt and M. Selke, *Dalton Trans.*, 2007, 3763–3770; (*e*) P.-G. Jensen, J. Arnbjerg, L. P. Tolbod, R. Toftegaard and P. R. Ogilby, *J. Phys. Chem. A*, 2009, **113**, 9965–9973.
35 S. Takizawa, T. Breitenbach, M. Westberg, L. Holmegaard, A. Gollmer, R. L. Jensen, S. Murata and P. R. Ogilby, *Photochem. Photobiol. Sci.*, 2015, **14**, 1831–1843.
36 (*a*) G. M. Sheldrick, *Acta Crystallogr.*, 1990, **A46**, 467; (*b*) G. M. Sheldrick, *SHELXTL, Bruker Analytical X-Ray Division*, Madison, 2001; (*c*) G. M. Sheldrick, *Acta Crystallogr., Sect. A: Fundam. Crystallogr.*, 2008, **64**, 112–122.
37 P. Brückner, W. Preetz and M. Pünjer, *Z. Anorg. Allg. Chem.*, 1997, **623**, 8–17.
38 T. Roisnel and J. Rodriguez-Carvajal, M. S. F. WinPLOTR: A Windows tool for powder diffraction patterns analysis, 378, 118–123. Recent developments of the program FULLPROF; Commission on powder diffraction (IUCr). Newsletter, 2001., WinPLOTR: A Windows tool for powder diffraction patterns analysis. Proceedings of the Seventh European Powder Diffraction Conference (EPDIC7), R. Delhez, E. J. Mittenmeijer, Eds.; Barcelona, Spain, May 20–23, 2000, vol. 118.
39 (*a*) R. D. Scurlock, D. O. Martire, P. R. Ogilby, V. L. Taylor and R. L. Clough, *Macromolecules*, 1994, **27**, 4787–4794; (*b*) J. Arnbjerg, M. Johnsen, P. K. Frederiksen, S. E. Braslavsky and P. R. Ogilby, *J. Phys. Chem. A*, 2006, **110**, 7375–7385; (*c*) P. Salice, J. Arnbjerg, B. W. Pedersen, R. Toftegaard, L. Beverina, G. A. Pagani and P. R. Ogilby, *J. Phys. Chem. A*, 2010, **114**, 2518–2525.
40 (*a*) R. Schmidt, C. Tanielian, R. Dunsbach and C. Wolff, *J. Photochem. Photobiol., A*, 1994, **79**, 11–17; (*b*) C. Martí, O. Jürgens, O. Cuenca, M. Casals and S. Nonell, *J. Photochem. Photobiol., A*, 1996, **97**, 11–18.
41 C. Franco and J. Olmsted, *Talanta*, 1990, **37**, 905–909.
42 J. M. Drake, M. L. Lesiecki and D. M. Camaioni, *Chem. Phys. Lett.*, 1985, **113**, 530–534.
43 K. Rurack and M. Spieles, *Anal. Chem.*, 2011, **83**, 1232–1242.

